Using a coherent hydrophone array for observing sperm whale range, classification, and shallow-water dive profiles

Duong D. Tran, Wei Huang, Alexander C. Bohn, and Delin Wang
Department of Electrical and Computer Engineering, Northeastern University, 360 Huntington Avenue, Boston, Massachusetts 02115

Zheng Gong and Nicholas C. Makris
Department of Mechanical Engineering, Massachusetts Institute of Technology, 77 Massachusetts Avenue, Cambridge, Massachusetts 02139

Purnima Ratilal[a)]
Department of Electrical and Computer Engineering, Northeastern University, 360 Huntington Avenue, Boston, Massachusetts 02115

(Received 17 September 2013; revised 20 February 2014; accepted 11 April 2014)

Sperm whales in the New England continental shelf and slope were passively localized, in both *range* and bearing, and classified using a single low-frequency (<2500 Hz), densely sampled, towed horizontal coherent hydrophone array system. Whale bearings were estimated using time-domain beamforming that provided high coherent array gain in sperm whale click signal-to-noise ratio. Whale ranges from the receiver array center were estimated using the moving array triangulation technique from a sequence of whale bearing measurements. Multiple concurrently vocalizing sperm whales, in the far-field of the horizontal receiver array, were distinguished and classified based on their horizontal spatial locations and the inter-pulse intervals of their vocalized click signals. The dive profile was estimated for a sperm whale in the shallow waters of the Gulf of Maine with 160 m water-column depth located close to the array's near-field where depth estimation was feasible by employing time difference of arrival of the direct and multiply reflected click signals received on the horizontal array. By accounting for transmission loss modeled using an ocean waveguide-acoustic propagation model, the sperm whale detection range was found to exceed 60 km in low to moderate sea state conditions after coherent array processing.
 [http://dx.doi.org/10.1121/1.4874601]

PACS number(s): 43.30.Pc, 43.30.Sf [AMT] Pages: 3352–3363

I. INTRODUCTION

Sperm whales (*Physeter macrocephalus*) in the Northwest Atlantic during spring and summer are concentrated along continental slope regions from the Mid-Atlantic Bight to south of Georges Bank (Whitehead *et al.*, 1992) and the Scotian shelf edge. While foraging, sperm whales perform deep dives lasting from several minutes to more than an hour (Watwood *et al.*, 2006), emitting short-duration broadband clicks with frequencies ranging from several hundred hertz to more than 30 kHz (Madsen *et al.*, 2002b; Weilgart and Whitehead, 1988). Each click exhibits a multi-pulse structure (Møhl, 2001; Norris and Harvey, 1972; Zimmer *et al.*, 2004) arising from reflections of the acoustic signal generated by the phonic lips off the frontal and distal air sacs bounding the spermaceti organ of a sperm whale. The inter-pulse interval (IPI) provides a measure of the length of the spermaceti organ that has been shown to be strongly correlated with the size of a sperm whale individual (Antunes *et al.*, 2010; Gordon, 1990; Growcott *et al.*, 2011; Mathias *et al.*, 2009; Miller *et al.*, 2013; Rhinelander and Dawson, 2004; Teloni *et al.*, 2007). Here we show that it is possible to distinguish and classify multiple vocalizing sperm whale individuals located in the far-field of a single, densely sampled, towed horizontal coherent hydrophone array system using the instantaneous sperm whale position estimates in both range and bearing, and the IPIs of the vocalized click signals. Most studies of the vocalization behavior and dive profile of sperm whales have been confined to deep continental slope environments bounding the Pacific and Atlantic ocean (Jacquet *et al.*, 2001; Madsen *et al.*, 2002b; Mathias *et al.*, 2012; Watwood *et al.*, 2006). Here we provide estimates of the three-dimensional (3D) dive profile of a sperm whale individual the vocalizations of which were opportunistically recorded in the shallow water environment of the Gulf of Maine with roughly 160 m water-column depth during a sea test of a newly developed, densely sampled, towed horizontal coherent receiver array system in May 2013.

Localization of an acoustic source, such as a vocalizing sperm whale, in the *far-field* of a *single,* densely sampled, towed horizontal coherent hydrophone array system is often a two-stage process. First, the bearing or horizontal direction of arrival of the acoustic signal is determined by time-delay analysis or beamforming of the signals received on the individual hydrophone elements of the array. Second, the range

[a)]Author to whom correspondence should be addressed. Electronic mail: purnima@ece.neu.edu

 0001-4966/2014/135(6)/3352/12/$30.00

or horizontal distance of the acoustic source from the receiver array center is determined by tracking changes in the bearing of a series of acoustic emissions over time (Gong *et al*., 2013; Nardone *et al*., 1984; Oshman, 1999; Ristic *et al*., 2004; Yardim *et al*., 2011). Short-aperture, towed horizontal coherent hydrophone array systems have been previously used to record vocalizations from sperm whales. However, the coherent receiver array data have only been applied to determine the bearing of a sperm whale. No subsequent *range* estimates have been made based solely on the coherent receiver array measurements. Consequently, coherent array gain of densely sampled hydrophone array systems has not been previously exploited for range localization of sperm whales. In Teloni (2005), a 128-element horizontal coherent hydrophone array system of the NATO Undersea Research Center (NURC) with an array aperture length of 11.6 m was employed to determine sperm whale vocalization bearings and to separate whale clicks from different azimuthal directions, but no range estimates or range analysis were provided. In Zimmer *et al*. (2004), click data from a single sperm whale acquired using the same NURC receiver array were used to determine the bearings of the whale individual. The sperm whale was primarily tracked using a digital tag (DTAG) attached to its body consisting of a hydrophone used to record sounds directly from the whale (Zimmer *et al*., 2004). The sperm whale range to the receiver array center was determined from click travel time difference between the DTAG hydrophone and the towed array hydrophones (Zimmer *et al*., 2004).

Here we localize multiple sperm whales in the far-field of a *single* low-frequency (<2.5 kHz), densely sampled, towed horizontal coherent hydrophone array system, providing estimates of both range and bearing for each sperm whale. Because no other acoustic sensors were available to us apart from the towed horizontal receiver array system, the whale ranges were estimated from their bearing-time trajectories. A review of methods that can be applied to passively estimate the range of an acoustic source from a single, densely sampled, towed horizontal coherent receiver array is provided in Sec. I of Gong *et al*. (2013). Here we employ the moving array triangulation technique developed in Gong *et al*. (2013) to estimate sperm whale ranges from the measured click bearings. This technique combines bearing measurements from spatially separated apertures of the towed horizontal coherent receiver array and employs the conventional triangulation ranging algorithm for localizing a source that may be in the near- or far-field of the array. Because data from only a single towed horizontal coherent receiver array are used here to remotely and passively localize both the range and bearing of sperm whales and to classify them, the methods and results developed here are highly relevant and can be directly applied to address the feasibility of monitoring sperm whales with other towed horizontal coherent receiver array systems, such as those employed in naval and geophysical applications, where it may be important and necessary to remotely sense marine mammal activity from long ranges. An advantage of bearings-only range localization with a densely sampled, towed horizontal coherent receiver array system is that no additional information about the environment, such as bathymetry or sound speed profile, is needed to estimate source range in the far-field of the array.

Other approaches for localizing sperm whales include (a) hyperbolic ranging with a small network of single hydrophones (Baggenstoss, 2011; Tiemann and Porter, 2003; Watkins and Schevill, 1972) and (b) time-delay measurement of click reflections from ocean boundaries acquired with a single hydrophone or a sparse array of hydrophones (Mathias *et al*., 2013; Mathias *et al*., 2012; Nosal and Frazer, 2006; Skarsoulis and Kalogerakis, 2006; Thode, 2004; Tiemann *et al*., 2006; Wahlberg, 2002). Here we utilize time difference of arrivals of the sperm whale direct and multiple bottom and surface reflected click [multiple-reflection based time difference of arrival (MR-TDA)] signals after beamforming to estimate the depth and hence the dive profile of a sperm whale in shallow waters of the Gulf of Maine with 160 m water-column depth. This sperm whale individual's horizontal range $r = 1$ km was very close to the array's near-field distance r_N ($r_N \leq L^2/\lambda \approx 750$ m, where L is the array aperture length and λ is the wavelength) making it possible to estimate its depth. Depth estimation for acoustic sources at long ranges, in the far-field ($r \gg L^2/\lambda$) of a single, *horizontal* coherent receiver array system is challenging because the acoustic wavefield received by the array is multi-modal in nature having undergone many surface and bottom bounces in a random ocean waveguide making the received field less sensitive to the source's depth location, except in the endfire direction of the horizontal array.

II. METHOD: EXPERIMENTAL DATA COLLECTION AND ANALYSIS

A newly developed, densely sampled, towed horizontal linear hydrophone array system funded by the National Science Foundation and the Office of Naval Research was deployed and tested in the continental slope region south of Cape Cod between 500 and 2000 m water depth on May 13 (site B in Fig. 1) and in the Gulf of Maine in 150–180 m water depth on May 14 and 15 (site A in Fig. 1). Passive acoustic data were collected on a sub-aperture of the array with $N = 32$ elements having an inter-element spacing of 0.75 m. The hydrophone elements, each having -188 dB re μPa/V sensitivity were sampled at 5 kHz with 24-bit digital resolution. The array was towed by the research vessel Endeavor at various speeds between 1 and 4 kn. The water-column sound speed at the experiment sites were monitored using a conductivity-temperature-depth (CTD) sensor and expendable bathythermographs (XBT). The measured sound speed profiles are shown in Fig. 2 for the two test sites. The array depth was maintained between 60 and 80 m near the thermocline in the Gulf of Maine, and varied between 10 and 50 m at the continental slope region.

To investigate the presence of sperm whale clicks, time-frequency spectrograms of the received signal on each hydrophone were first calculated, and the spectrogram incoherently averaged across several hydrophones were obtained. Sperm whale clicks were consistently present in all 75 min of passive acoustic recordings on May 13 at the continental

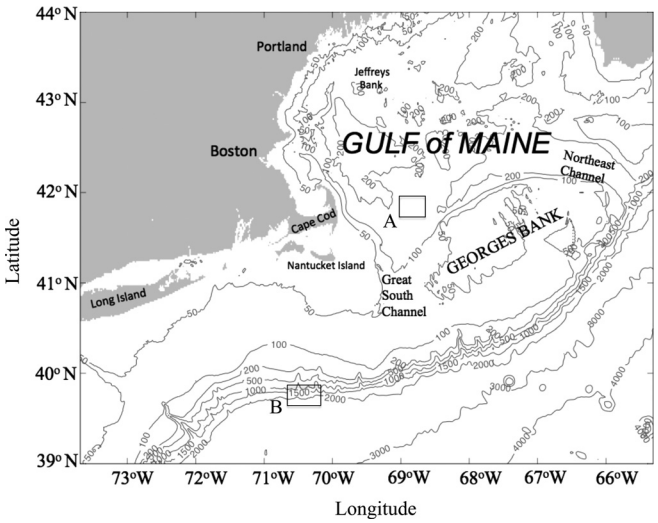

FIG. 1. Locations of the two test sites where the densely sampled, towed horizontal coherent receiver array was deployed to collect ambient noise data in May 2013. Site A is in the Gulf of Maine shallow water environment, and site B is in the deeper continental slope environment.

slope region and 1 h of passive acoustic recordings in the Gulf of Maine shallow waters. No active acoustic sound sources were used in the towed receiver array sea test.

The maximum frequency of the acoustic data recorded by the receiver array system here is 2.5 kHz. Our analysis of sperm whale clicks is therefore limited to the low-frequency component of the click signals in the several hundred hertz to a couple of kilohertz range that is more omnidirectional (Mathias *et al.*, 2013; Tiemann *et al.*, 2006; Zimmer *et al.*, 2004) and suffer less transmission loss. In contrast, the sampling frequencies of acoustic systems in previous sperm whale studies were significantly higher, by at least a factor of three (Mathias *et al.*, 2013; Tiemann *et al.*, 2006) to over ten times that used in this study to provide a more complete

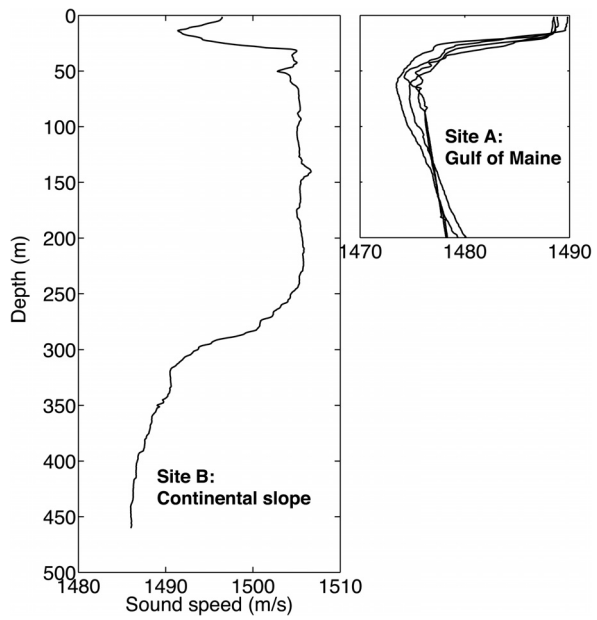

FIG. 2. Measured sound speed profiles at the two test sites shown in Fig. 1.

coverage of the bandwidth of the sperm whale click that can extend to 30 kHz (Madsen *et al.*, 2002a; Mathias *et al.*, 2012; Teloni, 2005; Thode, 2004; Watwood *et al.*, 2006; Zimmer *et al.*, 2004).

A. Sperm whale localization in horizontal range and azimuthal bearing

1. Determining click arrival time and azimuthal bearing

The relative horizontal azimuthal direction or relative bearing $\hat{\beta}'$ of each sperm whale click, measured from array broadside, was next estimated using time-domain delay-and-sum beamforming (Johnson and Dudgeon, 1993). The pressure-time series data from each hydrophone of the array were first high-pass filtered with 300 Hz cut-off frequency. Each two-dimensional (2D) matrix of high-pass filtered pressure-time series data from the 32 elements of the array within roughly 13 s duration was next converted to 2D beam-time data by steering the array in 400 azimuthal directions equally spaced from -1 to 1 in $\sin\beta'$, where β' is the azimuthal angle measured from array broadside. An angle of $\sin\beta' = -1$ corresponds to the back endfire direction and $\sin\beta' = 1$ corresponds to the forward endfire direction. The relative azimuthal direction and time of arrival of each sperm whale click were determined from the local peak energy levels of the 2D beam-time data. In general, the sperm whale clicks after high-pass filtering and beamforming stood between 10 and 35 dB above the background. A detection threshold of 10 dB above the background was applied in the local peak detection to reduce the false alarm rate.

Spectrogram and time-series examples of the beamformed received click trains are shown in Figs. 3 and 4. Because each sperm whale click contains multiple sharp pulses highly localized in time with a width of less than 1 ms per pulse (see Fig. 5), the click signal resembles the output of a matched filter. This enables high resolution beamforming in the time domain because coherent addition of the pulses across all hydrophones decorrelates within a small time lag of roughly 1/8 ms, corresponding to bearing estimation accuracies of approximately 1.7° at array broadside and 8° near array endfire. In contrast, the array angular resolution is much broader, roughly $\lambda/(L\cos\beta') = 3.7°$ at broadside and $2\sqrt{0.886\lambda/L} = 22.7°$ at endfire from planewave beamforming of a time-harmonic signal, where λ, L, and β' are, respectively, the wavelength, array aperture and azimuthal direction from array broadside (Johnson and Dudgeon, 1993; Makris *et al.*, 1995) for the given array aperture $L = 23.25$ m at a frequency of 2 kHz. Examples of the beam pattern obtained from beamforming two distinct sperm whale clicks, one located near array broadside and the other near array endfire are shown in Fig. 6. The direction of arrival is clearly distinguishable since the main lobe stands more than 8 dB above the grating lobe in both cases, mitigating any potential effect of spatial aliasing.

The estimated relative bearings $\hat{\beta}'$ measured with respect to array broadside were then converted to absolute bearings $\hat{\beta}$, measured from the array center with respect to true North by correcting for the corresponding array heading

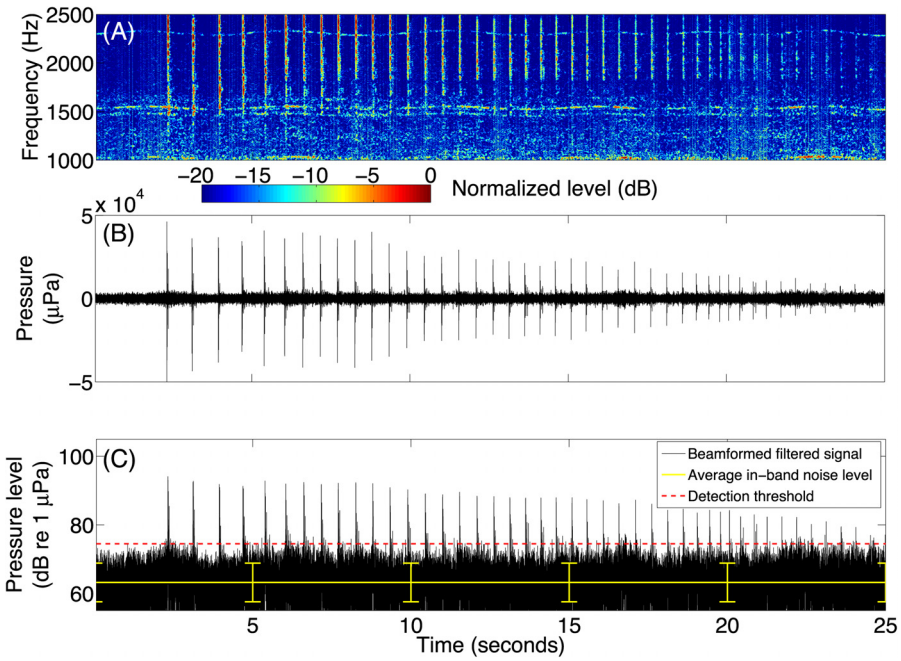

FIG. 3. (Color online) (A) Spectrogram of a series of sperm whale echolocation clicks recorded at frequencies up to 2.5 kHz in the Gulf of Maine on May 14 starting at 17:19:07 EDT. The spectrogram was calculated using a short-time Fourier transform with window size 256 and 75% overlap. (B) Beamformed pressure time series of the clicks, bandpass filtered between 1500 and 2500 Hz. (C) Beamformed pressure time series plotted in decibel (dB) scale. The solid curve with error bars shows the mean and standard deviation of beamformed background ambient noise level in the 1500–2500 Hz band, estimated from regions outside of clicks.

measurement α. To resolve the left-right ambiguity inherent in linear receiver array measurement of a source bearing, the left and right absolute bearing sequences were statistically correlated to the measured array headings. The true bearing sequence was selected to be the one with the smaller correlation coefficient because the ambiguous bearing sequence closely follows the array heading changes as shown in Fig. 2 of Gong *et al.* (2013). When the array is steered in the azimuth of sperm whale clicks, the array gain (Kay, 1998; Urick, 1983) obtained from coherent addition of the click signals measured across all $N = 32$ hydrophones can enhance the signal-to-noise ratio by approximately $10 \log_{10} N \approx 15$ dB over that of a single hydrophone [compare beamformed click signals in Fig. 4(C) with single hydrophone measured click

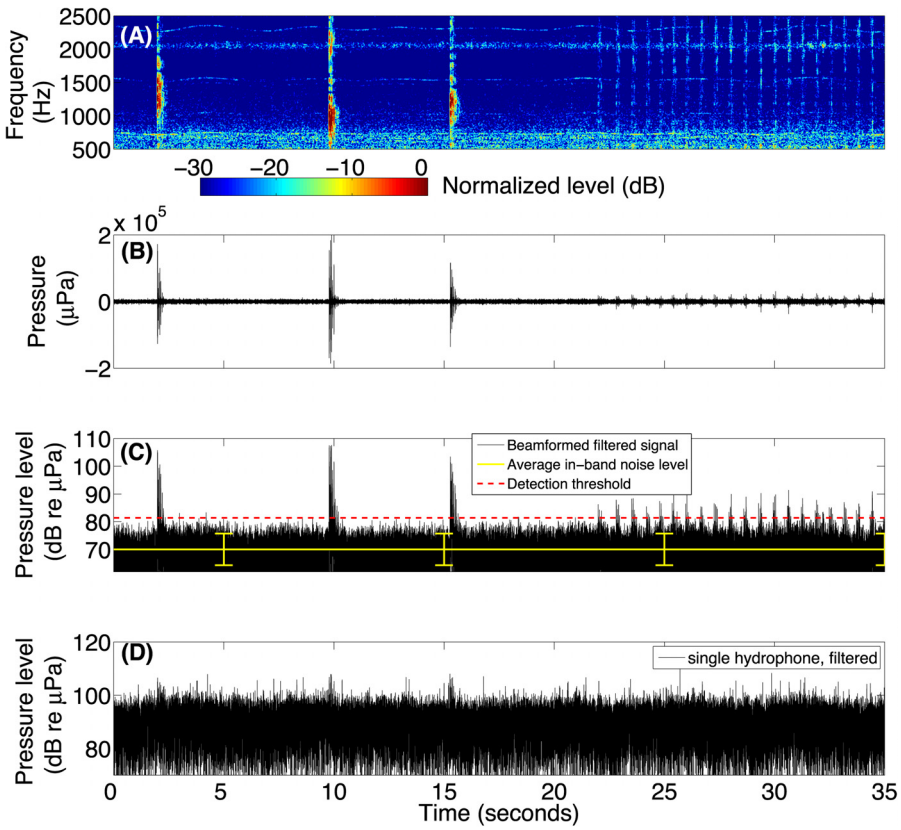

FIG. 4. (Color online) (A) Spectrogram of three consecutive slow clicks followed by a train of echolocation clicks recorded at frequencies up to 2.5 kHz in the Gulf of Maine on May 14 starting at 17:16:15 EDT. (B) Beamformed pressure time series of the clicks, bandpass filtered between 500 and 2500 Hz. (C) Beamformed pressure time series plotted in dB scale. The solid curve with error bars shows the mean and standard deviation of beamformed background ambient noise level in the 500–2500 Hz band, estimated from regions outside of clicks. (D) Corresponding signal received on a single hydrophone, bandpassed filtered between 500 and 2500 Hz.

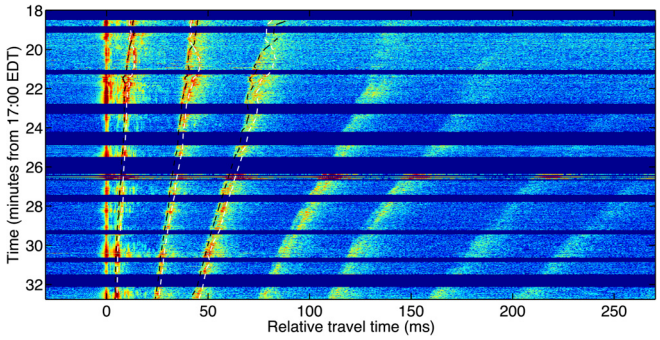

FIG. 5. (Color online) Multiple reflection arrival pattern of the sperm whale clicks detected on May 14 in the Gulf of Maine. The order of arrival is: Direct path; pairs of bottom and surface reflected, bottom-surface-bottom and surface-bottom-surface reflected, etc. Between 17:26:00 and 17:32:30 EDT, reflections from up to seven interface bounces are detected.

signals in Fig. 4(D)]. This significantly improves sperm whale click detectability and ranging capability. Note that an incoherent array of hydrophones also has no array gain over noise, regardless of the number of hydrophones, because coherence between sensors is necessary to accumulate array gain. Subsequent analyses on the temporal and spectral characteristics of the clicks were performed on the noise-suppressed beamformed clicks.

2. Range estimation for sperm whales in the near- or far-field of the towed horizontal coherent receiver array

Each sperm whale individual was localized and tracked from its corresponding sequence of click bearing measurements using the moving array triangulation (MAT) technique (Gong, 2012; Gong *et al.*, 2013), which combines bearing measurements from spatially separated apertures of a towed horizontal receiver array and employs the conventional triangulation ranging algorithm to localize a source in either the near- or far-field of the array. The whale range from the receiver array center was calculated using Eqs. (1) through (3) of Gong *et al.* (2013) given a pair of whale bearing measurements. The synthetic aperture length A_s created by the array

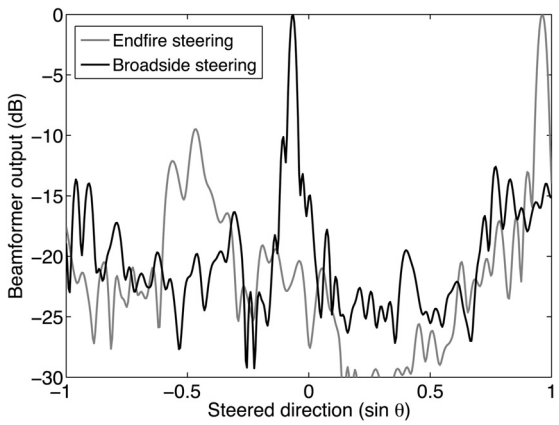

FIG. 6. Array beamformer output as a function of steering angle from array broadside 0° shown for two distinct time instances. Sperm whale clicks with relative bearing 3.7° near array broadside and 73.7° near array endfire. The corresponding 1-dB beamwidths are approximately 1.7° near broadside and 8.0° near endfire. Rectangular window was applied across the array aperture.

movement between pairs of whale bearing measurements in the MAT technique has to satisfy the near field condition, $A_s^2/\lambda \geq r_w$, where r_w is the whale range from the receiver center and λ is the wavelength of the click signal. To localize and track sperm whales at ranges less than 5 km from the array, with λ set to be 0.75 m, the synthetic aperture length should be at least 60 m. The array can be towed over this distance in half a minute, so that near real-time tracking of sperm whales is feasible with this method. To track sperm whales at longer ranges with the MAT technique, longer observation times would be necessary.

The sperm whale inter-click interval is approximately 1 s or less in a click train and the receiver array heading was updated at roughly 12 s intervals. The MAT technique was applied to pairs of click bearing measurements that were at least 12 s apart to estimate each whale range. The whale range estimates obtained here are expected to have smaller fractional errors than the MAT localization fractional errors reported in Gong *et al.* (2013). This is because, by the law of large numbers (Bertsekas and Tsitsiklis, 2002; Goodman, 1985), there are roughly six times more numerous range estimates derived from bearing measurements embedded in noise which can be regarded as statistically uncorrelated across time for the sperm whale problem compared to Gong *et al.* (2013) where only one range estimate was available at every 75 s interval for the source localization problem discussed there.

3. Simultaneous depth and range estimation for a sperm whale in shallow water

The range and depth of a sperm whale located approximately 1 km from the receiver array in the Gulf of Maine were simultaneously estimated using MR-TDA of beamformed direct and singly or multiply reflected click signals from sea bottom and surface. The concept for whale range and depth inference is similar to that presented in Thode *et al.* (2002). However, because the array depth was accurately known from depth sensor measurement sampled every 10 ms, there was one fewer unknown. As a result, only three arrivals: Direct path, bottom bounce, and surface bounce were required to solve for whale range and depth as derived and discussed in the appendix. When more than three arrivals were present, the localization result could be obtained with higher accuracy by employing all available information (see the appendix). The whale range estimates obtained using MR-TDA will be compared to those obtained with bearings-only MAT method in Sec. IV.

B. Inferring sperm whale size from IPIs

The first 10-15 ms of a sperm whale click usually consists of multiple pulses a few milliseconds apart (Backus and Schevill, 1966; Møhl, 2001; Møhl *et al.*, 2003; Norris and Harvey, 1972), resulting from multiple reflection within the whale head according to the bent-horn hypothesis (Norris and Harvey, 1972; Zimmer *et al.*, 2003, 2004). The IPI has been shown to correlate with the spermaceti length (Gordon, 1990; Rhinelander and Dawson, 2004) and with the overall body size (Antunes *et al.*, 2010; Growcott *et al.*, 2011;

Mathias *et al.*, 2009; Miller *et al.*, 2013; Teloni *et al.*, 2007). An automated moving local peak energy detector with a 1 ms averaging-time window was applied to the beamformed pressure-time series data to determine the arrival time of each pulse within a sperm whale click signal to estimate the IPI. The result for each click was plotted and visually inspected for accuracy. This analysis was applied to high-pass filtered beamformed pressure-time series data to suppress ambient noise and improve estimates of the IPI. Many click signals from each whale were examined, and only those with a clear multi-pulse structure were included in our analysis. IPI estimates were averaged over multiple clicks (roughly 20–60 per whale) to reduce the error in the IPI estimates. As can be noted from Table II, the standard deviation in the IPI estimates for each sperm whale is comparatively small, less than 10%. The whale body length, L_w, was then estimated here using the methods proposed by Gordon (1990) and Growcott *et al.* (2011)

$$L_{w,Gordon} = 4.833 + 1453 \times \text{IPI} - 0.001 \times \text{IPI}^2, \quad (1)$$

$$L_{w,Growcott} = 1.257 \times \text{IPI} + 5.736. \quad (2)$$

The sampling frequency of the towed array hydrophones limited our analysis of sperm whale click signal to frequencies $\leq$2.5 kHz. In this low-frequency regime, the sperm whale multipulsed-click signals are approximately omnidirectional.

C. Estimating sperm whale maximum detection range with the low-frequency towed coherent receiver array system

The maximum detection range of a sperm whale with our towed array system was determined as the range at which the transmission loss correction led to a received sperm whale click signal level that stood two standard deviations above the mean beamformed background noise level band-pass filtered between 300 Hz and 2.5 kHz. The two standard deviation signal excess enabled positive detection of sperm whales with over 95% confidence.

The broadband transmission loss from the sperm whale location to the receiver array was calculated at 10 Hz interval in the bandwidth of the received clicks using the parabolic equation-based range-dependent ocean waveguide-acoustic propagation model RAM (Collins, 1994). To simulate the effect of internal waves that randomized the acoustic propagation path, water-column sound speed profiles obtained from CTD and XBT measurements during the experiment were randomly updated every 500 m range, the approximate horizontal correlation length for linear internal waves. The bottom was assumed to be sandy with sound speed 1800 m/s, density 1800 kg/m^3 and attenuation 0.8 dB/λ. The water-column attenuation was set to 6×10^{-5} dB/λ. These waveguide parameters were previously found to provide the best-fit match between measured and modeled transmission loss in the Gulf of Maine (Andrews *et al.*, 2009; Gong *et al.*, 2010). The broadband transmission loss is obtained by incoherently averaging the received intensity from 50 Monte-Carlo realizations over the bandwidth of a sperm whale click from 1 to 2.5 kHz, following the approach of Andrews *et al.* (2009) and Gong *et al.* (2010).

III. RESULTS I: A SPERM WHALE IN SHALLOW WATERS OF THE GULF OF MAINE

A. Analysis of vocalizations

Vocalizations from a sperm whale individual at site A in the shallow-waters of the Gulf of Maine were recorded using the towed receiver array for over an hour from 16:35:00 to 17:40:00 EDT on May 14. An example of the beamformed time series and spectrogram of an echolocation click train is shown in Fig. 3. These measurements were made in water-column depths of roughly 160 m where the receiver array was located at roughly 65 m depth. The average inter-click interval was approximately 0.7 s; this implied that these clicks could be categorized as "usual clicks" (Whitehead and Weilgart, 1990). Spectrogram analysis indicates that the clicks contain significant energy at low frequencies in the 1.5–2.5 kHz range. This enabled the beamformed, high-pass filtered, time-series data of the clicks to stand between 15 and 30 dB above the mean background ambient noise level [Fig. 3(C)]. Click rates were found to vary within an echolocation click train, as shown in Fig. 3, where the inter-click intervals and click amplitudes decrease slowly over a time interval of about 20 s. This implied that the sperm whale vocalizations could be transitioning from clicks to creaks, which are a sequence of low energy clicks closely spaced in time emitted when homing in on a prey (Madsen *et al.*, 2002b; Miller *et al.*, 2004).

Besides these usual echolocation clicks, we also recorded intense broadband clicks with dominant energy contained in the 0.5-2 kHz frequency range. These loud clicks were separated by intervals of 5 s or longer (see Fig. 4) and can be categorized as slow clicks (Barlow and Taylor, 2005; Jacquet *et al.*, 2001; Oliveira *et al.*, 2013; Weilgart and Whitehead, 1993). The spectra of both the echolocation and slow clicks recorded here closely match those of DTAG-recorded sperm whale click vocalizations shown in Fig. 1 of Oliveira *et al.* (2013).

The occurrences of the recorded vocalizations are shown against time in Fig. 7 with click types indicated. Each echolocation click train lasted roughly 2 min with periods of silence varying between 20 s and several minutes. Longer periods of silence lasting between 5 and 10 min observed here may be associated with the sperm whale's ascent in the water-column (Zimmer *et al.*, 2004) and resting near the surface.

By analyzing each received click in the time interval from 17:18:00 to 17:33:00 EDT, we estimated the mean IPI for this sperm whale individual to be 3.0 ms with a standard deviation of 0.3 ms. This corresponds to a sperm whale length of approximately 9.3 m, according to Eq. (2).

B. Tracking range and depth of a sperm whale close to array near-field

The estimated bearings of the vocalizations obtained via time-domain beamforming are plotted in Fig. 7. The instantaneous sperm whale ranges were estimated from the

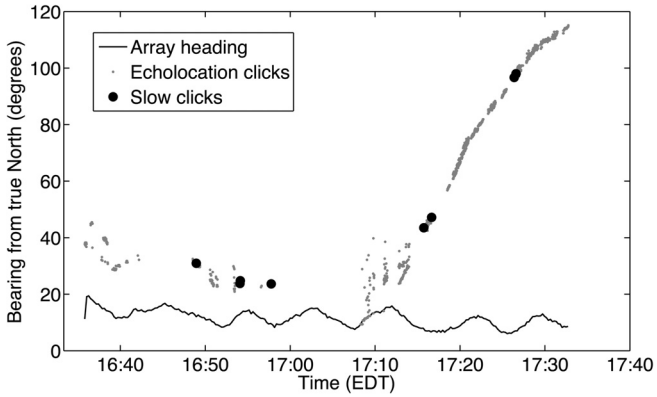

FIG. 7. Measured bearings of sperm whale echolocation and slow clicks detected in the Gulf of Maine on May 14 over a 1-h period from 16:35 to 17:35 EDT.

measured whale bearings using the bearings-only MAT technique for the time interval from 17:08:00 to 17:33:00 EDT and plotted in Fig. 8(A).

In the shallow water Gulf of Maine environment, clicks arriving at the receiver array from the sperm whale in close range to the array near-field distance display clear patterns of multiple reflection between the sea bottom and surface. The evolution of multipath arrival times is shown for all the clicks recorded between 17:18:00 and 17:33:00 EDT in Fig. 5. The direct arrival time of each click was first determined and aligned in time before the stacked sequence of clicks was created. Between 17:18:00 and 17:23:00 EDT, the first-order bottom and surface reflected arrivals are distinguishable in time, crossing each other due to vertical displacement of the whale. At other time instances, the bottom and surface reflections are not clearly distinguishable. The higher-order reflected arrivals are more prominent with shorter time separation for the later clicks in the time period analyzed. Multiple reflections in the shallow water waveguide extends the received sperm whale click time duration from 10-30 ms of the direct arrival (Møhl, 2001) to more than 250 ms.

The sperm whale range and depth were also simultaneously estimated by applying the MR-TDA technique described in the appendix for the time interval from 17:18:00 EDT to 17:33:00 EDT. All estimated delay times were used for each recorded click, giving a maximum of ${}^{7}C_{2} = 21$ range-depth estimates when seven reflections were detected, and a minimum of ${}^{4}C_{2} = 6$ range-depth estimates when four reflections were detected when employing the MR-TDA method. When ranges were available from the MAT technique, between four and seven depth-estimates could be obtained for each click, depending on the number of available reflections. The results are plotted in Fig. 8 comparing the MAT based results with the MR-TDA based results.

The analysis indicates that as the receiver array was being towed in the North bound direction, the sperm whale initially located roughly 0.5 km away from the array at 17:08:00 EDT moved away to a range of about 1.5 km in roughly 25 min. The whale appeared to hover within the water column without surfacing to breathe with estimated depth varying between 70 and 100 m over this time period. The increasing whale-receiver separation estimated using the MR-TDA explains the more compact arrival structure in Fig. 5 because when range increases, the reflection arrivals get closer to the direct path, as demonstrated in Fig. 12. The sperm whale range and depth estimates obtained via the MAT and MR-TDA methods agree well, especially near array broadside (between 17:23:00 and 17:28:00). At other time instances, the two methods yield results that are within 1 SD of each other. The whale range estimates obtained via MAT are expected to be more reliable than those obtained using MR-TDA. This is because in the MR-TDA technique, the whale range estimates depend on other parameters such as the unknown whale depth and water column depth. The range estimates obtained via MAT are not dependent on these parameters, instead it depends only on the measured bearing change of the whale with time.

C. Sperm whale detection range in shallow water

The click signals from this sperm whale located at roughly 1 km in range from the receiver array stood by as much as 35 dB over the mean background ambient noise level after beamforming [see Figs. 3(C) and 4(C)]. Because the background ambient noise level in the beam of the sperm whale after high pass filtering has roughly 5.5 dB standard

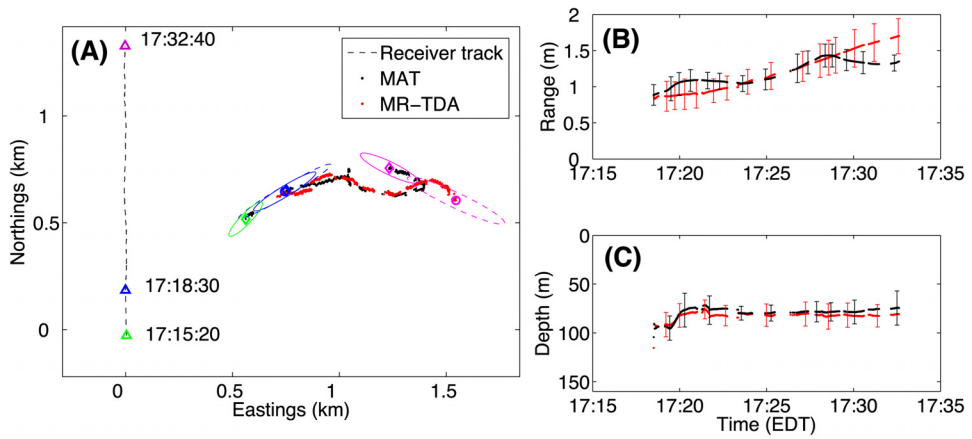

FIG. 8. (Color online) (A) Single sperm whale in Gulf of Maine localization result using the two methods, MAT and MR-TDA for the period between 17:15:20 and 17:32:40 EDT. The ellipses represent contours of localization uncertainty at each time instance with MAT (solid curve) and with MR-TDA (dashed curve). The origin of the coordinate system is located at (41°48.78′ N, 69°0.06′ W). (B) Range estimates using MAT and MR-TDA between 17:18:00 and 17:32:40 EDT. The error bars show the standard deviation of the range estimates in a 4-min time window. (C) Depth estimates for the same time period.

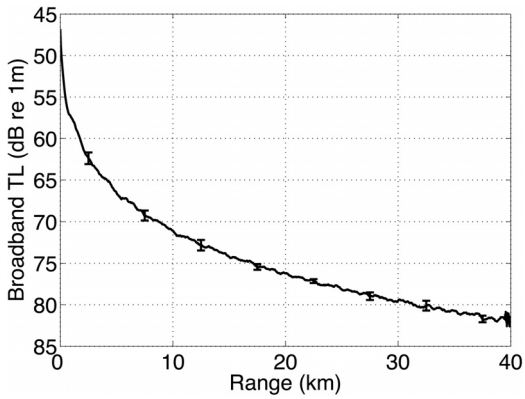

FIG. 9. Average broadband transmission loss in the frequency range of 1.5–2.5 kHz obtained using the RAM model at distances up to 80 km for the Gulf of Maine environment.

deviation, the sperm whale click signals have a signal excess of $(35\text{-}2 \times 5.5) = 24$ dB for our detector. The broadband transmission loss from a whale located approximately 1 km in range from the receiver array center and at a depth of 80 m is roughly 55 dB re 1 m [see Fig. 9(A)]. The signal excess of 24 dB implies that the sperm whale vocalizations can be detectable out to much longer ranges >60 km, where the transmission loss is $(55 + 24) = 79$ dB re 1 m, after beamforming with the towed receiver array. In contrast, sperm whale detection range with a single omnidirectional hydrophone is expected to be significantly limited [compare Fig. 4(C) showing the result after array beamforming with Fig. 4(D) which is the result for a single hydrophone]. Because sperm whale detection range is dependent on ambient noise level, the detection ranges given here are valid for low to moderate sea state of around two to three and wind speed between 8 and 11 kn, according to recorded measurements. The detection ranges will be larger at lower sea states and smaller at higher sea states.

IV. RESULTS II: MULTIPLE SPERM WHALES AT THE CONTINENTAL SLOPE SOUTH OF CAPE COD

We identified over 1000 sperm whale clicks in about 75 min of recording on May 13 at site B (Fig. 1) on the continental slope south of Cape Cod. Both left-right bearing estimates of the detected clicks are shown for roughly an hour of recording from 23:00:00 EDT on May 13 to 00:02:30 EDT on May 14 in Fig. 10. The left-right ambiguity of the linear receiver array is resolved for each group of clicks using the technique described in Sec. II A 1. The correlation coefficients between the change in bearings and the change in array headings for nine identified clusters of clicks in Fig. 10 are listed in Table I for both the left and right bearing candidates. A series of click bearings is determined to be true if (a) the correlation coefficient ρ is below 0.4, whereas the ambiguous group has $\rho > 0.6$, or (b) the correlation coefficient ρ is at least five times smaller than that of the ambiguous group. When none of these criteria are met, the true click bearings could not be determined and no localization result is obtained.

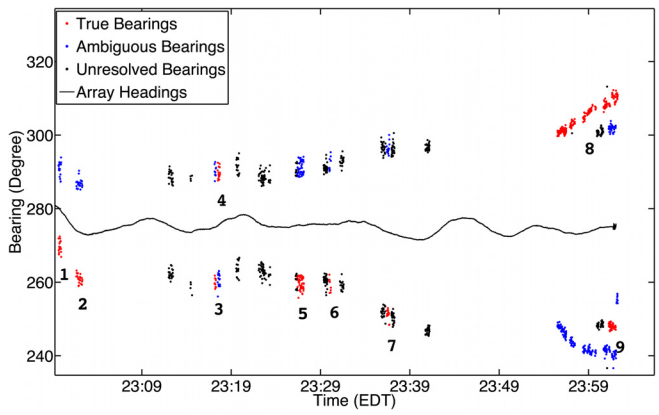

FIG. 10. (Color online) True and ambiguous bearings of sperm whale clicks received on the array on May 13 at site B on the continental slope. Whale bearings are grouped into clusters from 1 to 9 according to their temporal, spectral, and spatial characteristics.

TABLE I. Correlation coefficients between receiver array heading change and click bearing change for the candidate pairs of left-right absolute click bearing clusters shown in Fig. 10. The selected true click bearing clusters are each marked with an asterisk.

	Correlation coefficients, ρ		
Cluster	Right	Left	N
1	0.64	0.32*	17
2	0.66	0.36*	25
3	0.63	0.09*	10
4	0.09*	0.60	16
5	0.44	0.08*	41
6	0.64	0.34*	9
7	0.63	0.26*	17
8	0.37*	0.76	229
9	0.06*	0.27	42

A. Distinguishing sperm whale individuals using temporal, spectral, and spatial characteristics of clicks

We further associate the different click clusters to distinct sperm whale individuals based on the mean and standard deviation of IPI of each click cluster. The mean and standard deviation of the IPI as well as estimate of whale body length based on Eqs. (1) and (2) are provided in Table II for all

TABLE II. IPI for each cluster and the estimated sperm whale body length.

Cluster number	$\langle IPI \rangle$ (ms)	σ_{IPI} (ms)	$L_{w,Gordon}$ (m)	$L_{w,Growcott}$ (m)	Whale group	N
1	3.4	0.4	9.8	10.0	A	10
2	7.7	0.7	16.0	15.4	B	8
3	3.3	0.3	9.6	9.9	A	8
4	4.2	0.3	11.0	11.0	C	11
5	4.3	0.2	11.0	11.1	C	9
6	7.6	0.7	15.8	15.3	B	5
7	4.9	0.3	11.9	12.0	D	12
8-1	4.7	0.3	11.6	11.6	E	43
8-2	4.6	0.3	11.5	11.5	E	12
8-3	4.5	0.4	11.4	11.4	E	18
8-4	4.5	0.4	11.4	11.4	E	33
9	6.9	0.5	14.8	14.4	F	17

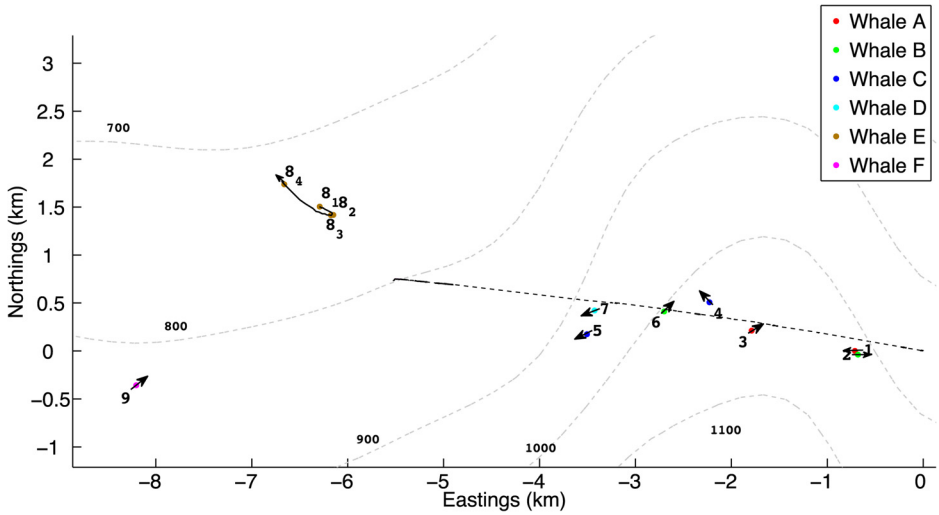

FIG. 11. (Color online) Localization and tracking result for multiple sperm whales with bearing clusters shown in Fig. 10 on May 13 at site B on the continental slope. The dashed curve is the track of the receiver array. The origin of the coordinate system is located at (39°50.94′ N, 70°19.55′ W).

identified click clusters. Based on the measured IPI, we associate click clusters 1 and 3 (mean IPI ≈ 3.4 ms) to the same whale A. Similarly, click clusters 2 and 6 are associated with whale B with much longer IPI of approximately 7.6 ms. Whale C is associated with click clusters 4 and 5. Click cluster 9 has very distinct IPI and corresponding whale size estimate and is associated with whale F. Whale D is associated with click cluster 7, while whale E is assumed to possess the IPI measurement of click cluster 8, which is composed of sub-clusters 8-1, 8-2, 8-3 and 8-4. The IPI values measured for clusters associated with whale E lie between those of whale C and whale D, so whale E could also possibly be either C or D. From Table II, the estimated number of sperm whale individuals simultaneously and passively recorded by the towed receiver array is at least 4 or as many as 6.

B. Localization and tracking of multiple sperm whales in far-field of the towed horizontal coherent receiver array

The sperm whale click clusters from May 13 are localized using the bearings-only MAT technique and the results are shown in Fig. 11 grouped according to the classification and association results obtained in Sec. IV A. Whale A

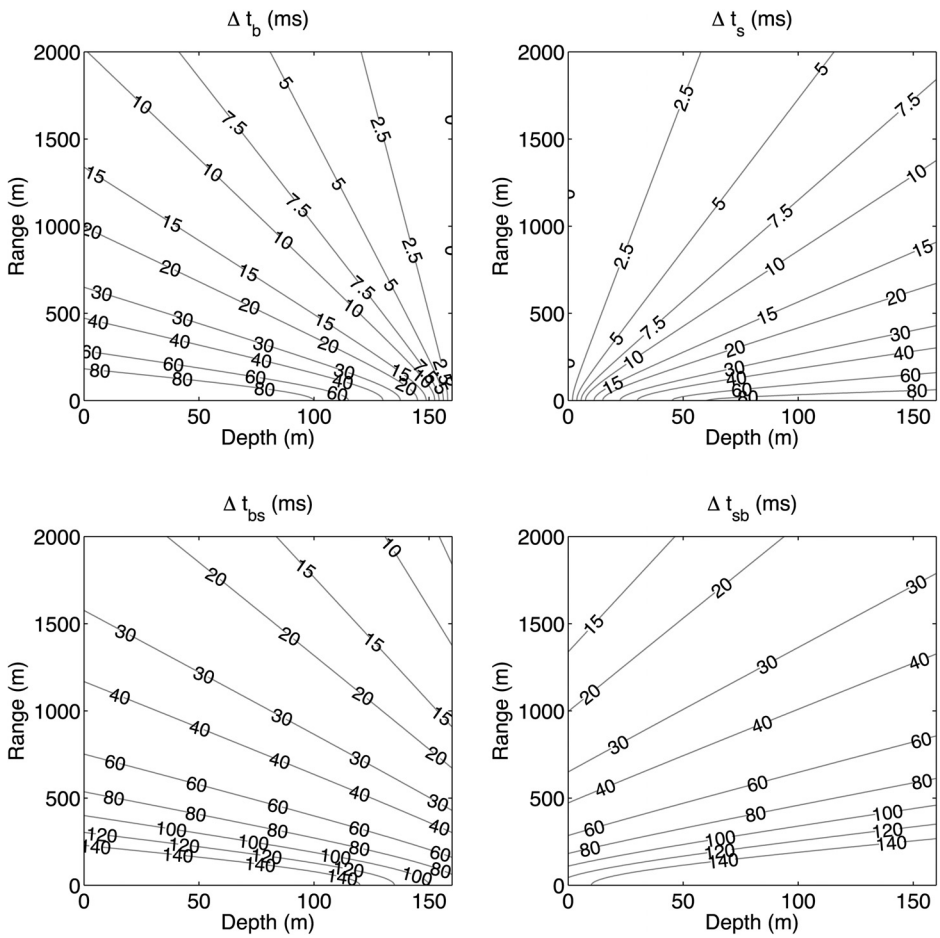

FIG. 12. Calculated time delays from direct arrival for the bottom bounce Δt_b (upper left), surface bounce Δt_s (upper right), bottom-surface bounces Δt_{bs} (lower left), and surface-bottom bounces Δt_{sb} (lower right) as a function of whale range and depth. The receiver depth is set at 65 m and the water depth is 160 m.

(clusters 1 and 3) moves west a distance of about 1.1 km in a time interval of 17 min at a mean speed of roughly 1.1 m/s. Whale B (clusters 2 and 6) also moves west 2 km in 28 min, at a speed of approximately 1.2 m/s. Whale C (clusters 4 and 5) moves about 1.3 km in 10 min at a speed of 2 m/s. Whale D (cluster 7) is associated with a short period of clicking, and therefore no detailed movement tracking is available, although we can deduce that it is moving in the southwest direction. Whale E (cluster 8) has IPI values close to that of both whale C and D, however the localization results show that this whale is further to the Northwest of the receiver, and several kilometers away from both whales C and D. Whale F has distinct spectral and temporal characteristics demonstrated by low ICI and high IPI and is localized to the southwest of the receiver toward the end of the track.

V. CONCLUSION

Sperm whales in the New England continental shelf and slope have been passively localized, in both range and bearing, tracked, and classified using a single low frequency (<2500 Hz), densely sampled, towed horizontal coherent receiver array system. Coherent array gain, which increases sperm-whale-click-signal-to-background-noise ratio, was exploited to first determine the sperm whale bearing or horizontal direction by time-domain beamforming, and next estimate the sperm whale range or horizontal distance to the receiver array center by the moving array triangulation technique. Multiple concurrently vocalizing sperm whales were distinguished and classified based on their horizontal spatial location and the IPIs of their click signals, which is highly correlated to sperm whale body length. The vast majority of sperm whales were located in the far-field of the horizontal receiver array system. An advantage of bearings-only range localization with a densely sampled, towed horizontal coherent receiver array system is that no additional information about the environment, such as bathymetry or sound speed profile, is needed to estimate source range in the far-field of the array.

While studies have focused on examining the function of sperm whale clicks and their behavior during their descent in deep waters (Jacquet *et al.*, 2001; Madsen *et al.*, 2002b; Miller *et al.*, 2004; Oliveira *et al.*, 2013), their behaviors in shallow water are not well understood due to the fact that sperm whales are not common in this environment. Here the depth profile is estimated for a sperm whale in the shallow waters of the Gulf of Maine with 160 m water-column depth. This whale was located close to the near-field distance of the horizontal coherent receiver array system enabling its depth to be estimated from time-of-arrival-differences of the direct and the multiply reflected click signal. Over a roughly 15 min time interval analyzed in this paper, this sperm whale swam a horizontal distance of over 500 m, emitting both echolocation and slow clicks, while being entirely submerged and hovering close to the mid-water column.

The densely sampled, towed horizontal coherent receiver array system employed here is similar to that used in naval operations for long range ocean surveillance and in geophysical exploration. It may be important and necessary to remotely sense marine mammal activity from long ranges in these applications. The methods developed here and the results obtained here can be directly applied to assess the performance of these other coherent receiver array systems for monitoring sperm whales from long ranges.

ACKNOWLEDGMENTS

This work was funded by the National Science Foundation and the Office of Naval Research. The authors would like to thank Scott Whitney of BAE Systems, Carl Stevens of Einhorn Engineering, and the staff and crew of RV Endeavor for assistance with the data collection.

APPENDIX: SIMULTANEOUS RANGE-DEPTH LOCALIZATION USING MR-TDA

A formulation and an analytic solution are first provided for simultaneous range-depth localization of a sperm whale using delay times of the two first-order reflections of its click from the sea surface and bottom. Next, a method incorporating all detected reflections, including higher-order reflections from sea surface and bottom is presented. This latter method can enhance localization accuracy and reduce errors associated with estimating click reflection delay times.

Let the known receiver array center depth be z_r, and the unknown whale range and depth be r_w and z_w, respectively. Let H be the water depth that is assumed to be constant within the propagation path from the whale to the receiver. The sound speed variation with depth and range is assumed to cause negligible refraction given the short propagation path from the sperm whale to receiver. The direct, first-, and second-order reflected path lengths from the vocalizing whale to the receiver are

$$\text{Direct path}: \quad d = \sqrt{r_w^2 + (z_r - z_w)^2}, \tag{A1}$$

$$\text{Surface-reflected}: \quad s = \sqrt{r_w^2 + (z_r + z_w)^2}, \tag{A2}$$

$$\text{Bottom-reflected}: \quad b = \sqrt{r_w^2 + (2H - z_r - z_w)^2}, \tag{A3}$$

$$\text{Surface-bottom reflected}: sb = \sqrt{r_w^2 + (2H + z_w - z_r)^2}, \tag{A4}$$

$$\text{Bottom-surface reflected}: bs = \sqrt{r_w^2 + (2H - z_w - z_r)^2}. \tag{A5}$$

Because there are only two unknowns r_w and z_w, only two time delays are needed to estimate these unknowns. We choose the two first-order surface-reflected and bottom-reflected arrivals as they often encounter the least losses and are therefore easier to detect. The difference in arrival times are

$$\Delta t_s = \frac{s - d}{c} = \frac{4z_r}{c(2d + \Delta t_s)}, \tag{A6}$$

$$\Delta t_b = \frac{b-d}{c} = \frac{4(H-z_r)(H-z_w)}{c(2d+\Delta t_b)}, \tag{A7}$$

which can be combined into

$$\begin{bmatrix} -2c\Delta t_s & 4z_r \\ -2c\Delta t_b & -4(H-z_r) \end{bmatrix} \begin{bmatrix} d \\ z_w \end{bmatrix} = \begin{bmatrix} c(\Delta t_s)^2 \\ c(\Delta t_b)^2 - 4(H-z_r)H \end{bmatrix}, \tag{A8}$$

where c is the mean sound speed in the water-column. Using the time delay of the first-order surface and bottom reflected arrivals, Δt_s and Δt_b, as inputs, the range and depth of the whale can be calculated via

$$\begin{bmatrix} d \\ z_w \end{bmatrix} = \begin{bmatrix} -2c\Delta t_s & 4z_r \\ -2c\Delta t_b & -4(H-z_r) \end{bmatrix}^{-1} \times \begin{bmatrix} c(\Delta t_s)^2 \\ c(\Delta t_b)^2 - 4(H-z_r)H \end{bmatrix}, \tag{A9}$$

$$r_w = \sqrt{d^2 - (z_r - z_w)^2}. \tag{A10}$$

When more than three arrivals are present, the time delays for each order of multiple reflection can be calculated as a function of candidate source ranges and source depths given the water depth and receiver depth as inputs. Suppose a time delay $\Delta t_b = t_0$ is measured for the first bottom reflection. A unique contour then exists for the set of range and depth combination $\{r_w, z_w\}$ such that $\Delta t_b = t_0$. This is illustrated in Fig. 12 for various delays between 0 and 80 ms. Similarly, constant time delay contours can be constructed for the surface bounce, bottom-surface bounces, surface-bottom bounces (see Fig. 12), and other higher order multiple reflections. If two time delay measurements are available, an estimate of the whale location can be obtained at the intersection of the two contours. When the two time delays are the first-order reflections from ocean bottom and surface, this is equivalent to solving Eq. (A9). When N time-delays are available, the number of contour intersections is

$$\binom{N}{2} = N(N-1)/2,$$

which corresponds to the number of independent range-depth estimates based on time delay pairs. The solution is then taken to be the mean range and depth obtained from averaging these independent estimates.

In the shallow Gulf of Maine environment ($H < 200$ m), multiple reflections from the sea bottom and surface are only distinguishable from the direct arrival at small ranges approximately within a couple of kilometers. At longer ranges, the time difference of arrival of the direct and first-order interface reflections Δt_b and Δt_s becomes smaller and negligible with increasing range as shown in Fig. 12. When the whale is far away from the receiver, only higher order reflections are separable in time from the direct path; however, they suffer higher transmission losses due to multiple bottom and surface interaction and are difficult to detect (see Fig. 1 of Thode *et al.*, 2002). The small range also guarantees that the water depth H is relatively unchanged along the acoustic propagation path from whale to receiver.

1. Depth-localization when range information is available

When the range of a sperm whale can be estimated using an independent method, such as the MAT, the MR-TDA problem has reduced dimensionality because only the whale depth needs to be estimated. Figure 12 shows that a unique depth solution exists for each click reflection delay time measurement at a particular range. The whale depth is then estimated as the average of the N independent depth estimates from N reflected click time delays.

Andrews, M., Chen, T., and Ratilal, P. (**2009**). "Empirical dependence of acoustic transmission scintillation statistics on bandwidth, frequency, and range in New Jersey continental shelf," J. Acoust. Soc. Am. **125**, 111–124.

Antunes, R., Rendell, L., and Gordon, J. (**2010**). "Measuring inter-pulse intervals in sperm whale clicks: Consistency of automatic estimation methods," J. Acoust. Soc. Am. **127**, 3239–3247.

Backus, R. H., and Schevill, W. E. (**1966**). "Physeter clicks," in *Whales, Dolphins and Porpoises* (University of California Press, Berkeley, CA), pp. 510–527.

Baggenstoss, P. M. (**2011**). "An algorithm for the localization of multiple interfering sperm whales using multi-sensor time difference of arrival," J. Acoust. Soc. Am. **130**, 102–112.

Barlow, J., and Taylor, B. L. (**2005**). "Estimates of sperm whale abundance in the Northeastern temperate Pacific from a combined acoustic and visual survey," Mar. Mamm. Sci. **21**, 429–445.

Bertsekas, D. P., and Tsitsiklis, J. N. (**2002**). *Introduction to Probability*, 1st ed. (Athena Scientific, Belmont, MA), pp. 1–430.

Collins, M. D. (**1994**). "Generalization of the Split-Step Padé solution," J. Acoust. Soc. Am. **96**, 382–385.

Gong, Z. (**2012**). "Remote sensing of marine life and submerged target motions with ocean waveguide acoustics," Ph.D. dissertation, Northeastern University, Boston, MA.

Gong, Z., Andrews, M., Jagannathan, S., Patel, R., Jech, J., Makris, N. C., and Ratilal, P. (**2010**). "Low-frequency target strength and abundance of shoaling Atlantic herring (*Clupea harengus*) in the Gulf of Maine during the Ocean Acoustic Waveguide Remote Sensing 2006 Experiment," J. Acoust. Soc. Am. **127**, 104–123.

Gong, Z., Tran, D. D., and Ratilal, P. (**2013**). "Comparing passive source localization and tracking approaches with a towed-horizontal receiver array in an ocean waveguide," J. Acoust. Soc. Am. **134**, 3705–3720.

Goodman, J. W. (**1985**). *Statistical Optics* (Wiley, New York), pp. 1–572.

Gordon, J. C. D. (**1991**). "Evaluation of a method for determining the length of sperm whales (*Physeter catodon*) from their vocalizations," J. Zool. Lond. **224**, 301–314.

Growcott, A., Miller, B., Sirguey, P., Slooten, E., and Dawson, S. (**2011**). "Measuring body length of male sperm whales from their clicks: The relationship between inter-pulse intervals and photogrammetrically measured lengths," J. Acoust. Soc. Am. **130**, 568–573.

Jacquet, N., Dawson, S., and Douglas, L. (**2001**). "Vocal behavior of male sperm whales: Why do they click?," J. Acoust. Soc. Am. **109**, 2254–2259.

Johnson, D. H., and Dudgeon, D. E. (**1993**). *Array Signal Processing: Concepts and Techniques* (Prentice Hall, Upper Saddle River, NJ), pp. 1–512.

Kay, S. (**1998**). *Fundamentals of Statistical Signal Processing. II. Detection Theory* (Prentice Hall, Upper Saddle River, NJ), p. 512.

Madsen, P. T., Payne, R., Kristiansen, N. U., Wahlberg, M., Kerr, I., and Møhl, B. (**2002a**). "Sperm whale sound production studied with ultrasound time/depth-recording tags," J. Exp. Biol. **205**, 1899–1906.

Madsen, P. T., Wahlberg, M., and Møhl, B. (**2002b**), "Male sperm whale (*Physeter macrocephalus*) acoustics in a high-latitude habitat: Implications for echolocation and communication," Behav. Ecol. Sociobiol **53**, 31–41.

Makris, N. C., Avelino, L. Z., and Menis, R. (**1995**). "Deterministic reverberation from ocean ridges," J. Acoust. Soc. Am. **97**, 3547–3574.
Mathias, D., Thode, A., Straley, J., and Folkert, K. (**2009**). "Relationship between sperm whale (*Physeter macrocephalus*) click structure and size derived from video-camera images of a depredating whale (sperm whale prey acquisition)," J. Acoust. Soc. Am. **125**, 3444–3543.
Mathias, D., Thode, A. M., Straley, J., and Andrews, R. D. (**2013**). "Acoustic tracking of sperm whales in the Gulf of Alaska using a two-element vertical array and tags," J. Acoust. Soc. Am. **134**, 2446–2461.
Mathias, D., Thode, A. M., Straley, J., Calambokidis, J., Schorr, G. S., and Andrews, R. D. (**2012**). "Acoustic and diving behavior of sperm whales (*Physeter macrocephalus*) during natural and depredation foraging in the Gulf of Alaska," J. Acoust. Soc. Am. **132**, 518–532.
Miller, B. S., Growcott, A., Slooten, E., and Dawson, S. M. (**2013**). "Acoustically derived growth rates of sperm whales (*Physeter macrocephalus*) in Kaikoura, New Zealand," J. Acoust. Soc. Am. **134**, 2438–2445.
Miller, P. J. O., Johnson, M. P., and Tyack, P. L. (**2004**). "Sperm whale behaviour indicates the use of echolocation click buzzes 'creaks' in prey capture," Proc. R. Soc. Lond. B **271**, 2239–2247.
Møhl, B. (**2001**). "Sound transmission in the nose of the sperm whale (*Physeter catodon*). A post mortem study," J. Comp. Physiol. **187**, 335–340.
Møhl, B., Wahlberg, M., Madsen, P. T., Heerfordt, A., and Lund, A. (**2003**). "The monopulsed nature of sperm whale clicks," J. Acoust. Soc. Am. **114**, 1143–1154.
Nardone, S. C., Lindgren, A. G., and Gong, K. F. (**1984**). "Fundamental properties and performance of conventional bearings-only target motion analysis," IEEE Trans. Autom. Control **29**, 775–787.
Norris, K. S., and Harvey, G. W. (**1972**). "A theory for the function of the spermaceti organ of the sperm whale," NASA Special Publication 262 (Washington, DC), pp. 397–416.
Nosal, E.-M., and Frazer, L. N. (**2006**). "Track of a sperm whale from delays between direct and surface-reflected clicks," Appl. Acoust. **67**, 1187–1201.
Oliveira, C., Wahlberg, M., Johnson, M., Miller, P. J., and Madsen, P. T. (**2013**). "The function of male sperm whale slow clicks in a high latitude habitat: Communication, echolocation, or prey debilitation?," J. Acoust. Soc. Am. **133**, 3135–3144.
Oshman, Y. (**1999**). "Optimization of observer trajectories for bearings-only target localization," IEEE Trans. Aerosp. Electron. Syst. **35**, 892–902.
Rhinelander, M. Q., and Dawson, S. M. (**2004**). "Measuring sperm whales from their clicks: Stability of interpulse intervals and validation that they indicate whale length," J. Acoust. Soc. Am. **115**, 1826–1831.
Ristic, B., Arulampalam, S., and Gordon, N. (**2004**). *Beyond the Kalman Filter: Particle Filters for Tracking Applications* (Artech House, Norwood, MA), pp. 1–153.
Skarsoulis, E. K., and Kalogerakis, M. A. (**2006**). "Two-hydrophone localization of a click source in the presence of refraction," Appl. Acoust. **67**, 1202–1212.
Teloni, V. (**2005**). "Patterns of sound production in diving sperm whales in the Northwestern Mediterranean," Mar. Mamm. Sci. **21**, 446–457.
Teloni, V., Zimmer, W. M. X., Wahlberg, M., and Madsen, P. T. (**2007**). "Consistent acoustic size estimation of sperm whales using clicks recorded from unknown aspects," J. Cetacean Res. Manage. **9**, 127–136.
Thode, A. (**2004**). "Tracking sperm whale (*Physeter macrocephalus*) dive profiles using a towed passive acoustic array," J. Acoust. Soc. Am. **116**, 245–253.
Thode, A., Mellinger, D. K., Stienessen, S., Martinez, A., and Mullin, K. (**2002**). "Depth-dependent acoustic features of diving sperm whales (*Physeter macrocephalus*) in the Gulf of Mexico," J. Acoust. Soc. Am. **112**, 308–321.
Tiemann, C. O., and Porter, M. B. (**2003**). "Automated model-based localization of sperm whale clicks," *Proceedings of OCEANS 2003*, Vol. 2, pp. 821–827.
Tiemann, C. O., Thode, A. M., Straley, J., O'Connell, V., and Folkert, K. (**2006**). "Three-dimensional localization of sperm whales using a single hydrophone," J. Acoust. Soc. Am. **120**, 2355–2365.
Urick, R. J. (**1983**). *Principles of Underwater Sound* (McGraw-Hill, New York), pp. 29–65 and 343–366.
Wahlberg, M. (**2002**). "The acoustic behaviour of diving sperm whales observed with a hydrophone array," J. Exp. Mar. Biol. Ecol. **281**, 53–62.
Watkins, W. A., and Schevill, W. E. (**1972**). "Sound source location by arrival times on a non-rigid three dimensional hydrophone array," Oceanogr. Abstr. **19**, 691–692.
Watwood, S. L., Miller, P. J. O., Johnson, M., Madsen, P. T., and Tyack, P. L. (**2006**). "Deep-diving foraging behaviour of sperm whales," J. Anim. Ecol. **75**, 814–825.
Weilgart, L. and, Whitehead, H. (**1993**). "Coda communication by sperm whales (*Physeter Macrocephalus*) off the Galapagos Islands," Can. J. Zool. **71**, 744–752.
Weilgart, L. S., and Whitehead, H. (**1988**). "Distinctive vocalizations from mature male sperm whales (*Physeter macrocephalus*)," Can. J. Zool. **66**, 1931–1937.
Whitehead, H., Brennan, S., and Grover, D. (**1992**). "Distribution and behaviour of male sperm whales on the Scotian Shelf, Canada," Can. J. Zool **70**, 912–918.
Whitehead, H., and Weilgart, L. (**1990**). "Click rates from sperm whales," J. Acoust. Soc. Am. **87**, 1798–1806.
Yardim, C., Michalopoulou, Z., and Gerstoft, P. (**2011**). "An overview of sequential Bayesian filtering in ocean acoustics," IEEE J. Ocean. Eng. **36**, 71–89.
Zimmer, W. M. X., Johnson, M., D'Amico, A., and Tyack, P. L. (**2003**). "Combining data from a multisensor tag and passive sonar to determing the diving behavior of a sperm whale (*Physeter macrocephalus*)," IEEE J. Ocean. Eng. **28**, 13–28.
Zimmer, W. M. X., Tyack, P. L., Johnson, M. P., and Madsen, P. T. (**2005**). "Three-dimensional beam pattern of regular sperm whale clicks confirms bent-horn hypothesis," J. Acoust. Soc. Am. **117**, 1473–1485.